

Fitting of a Closed Planar Curve Representing a Profile of an Archaeological Fragment *

Kateřina Hlaváčková-Schindler,
Martin Kampel, and Robert Sablatnig

Pattern Recognition and Image Processing Group

Institute of Computer Aided Automation, Vienna University of Technology,

Favoritenstraße 9/1832, A-1040 Vienna, Austria

Fax: +43(1)58801-18392; e-mail: {kat,kampel,sab}@prip.tuwien.ac.at

Abstract

Motivated by the requirements of the present archaeology, we are developing an automated system for archaeological classification of ceramics. The basis for classification and reconstruction of ceramics is the profile, which is the cross-section of the fragment in the direction of the rotational axis of symmetry, and can be represented by a closed curve in the plane. This paper compares and combines several methods for interpolation and approximation of a closed curve by B -splines in the plane. The closed curve, representing the profile, is divided into several parts for which the most accurate method is selected. All the interpolation and approximation methods are compared on the provided data with respect to the achieved precision and 'complexity' of the curve description. The graphical output of the program suggests to the archaeologists, which combination of these methods gives the best representation of the reconstructed profile from the data under the smallest possible error and the simplest possible spline representation.

1 Introduction

Ceramics are among of the most widespread archaeological finds, having a short-period of use. Since the 19th century, the physical characteristics of archaeological pottery have been used to assess cultural groups, population movements, inter-regional contacts, production contexts, and technical or functional constraints (archaeometry). Because archaeometry of pottery still suffers from a lack of methodology, it is important to develop analytical classification tools of artifacts [26]. A large number of ceramic fragments, called sherds, are found at every excavation. These fragments are documented by being photographed, measured, and drawn; then they are classified. The purpose of *classification* is to get a systematic

view on the excavation finds. Archaeological finds are traditionally grouped by typology [12]. Defined forms and types of vessels form codes which simplify communication within the scientific field. Figure 1 is a representative of other examples.

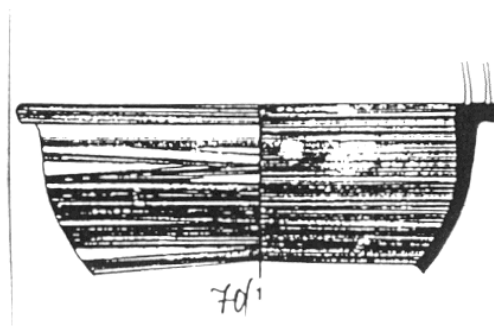


Figure 1: Drawing of a complete pot.

The drawing and interpretation of ceramic fragments is very time consuming and costly work, requiring trained and qualified draftsmen. A graphic documentation done by hand also increases the possibility of errors. Converting the pencil drawing into an ink drawing is another potential source of error. There may be errors in the measuring process (diameter or height may be inaccurate), and inconsistencies in the drawing of the fragment. However it is not possible to achieve a consistent style, since it is very difficult to make a drawing of an object without interpreting it. This leads to a lack of objectivity in the documentation of the material.

Because the conventional documentation methods were shown to be unsatisfactory [26], the interest in finding any automatic solution increased (see [13],[33],[32] for some examples). None of the developed systems could satisfy the requirements of the archaeologists since the amount of the acquisition work did not reduce. Our automated 3d-object acquisition system was developed to satisfy the above mentioned archaeological requirements [29]. The profile sections are achieved automatically by a 3D-measurement system based on

* This work was supported in part by the Austrian Science Foundation (FWF) under grant P13385-INF, the European Union under grant IST-1999-20273 and the Austrian Federal Ministry of Education, Science and Culture.

structured (coded) light and two lasers technique. Shape from structured light is a method which constructs a surface model of an object based on projecting a sequence of well defined light patterns onto the object. An image of the scene is taken for every pattern. This image, together with the knowledge about the pattern and its relative position to the camera are used to calculate the coordinates of points belonging to the surface of the object ([19], [20]).

Up to the present, traditional methods of classification of archaeological pottery have been applied (see [2, 1, 3, 6, 8, 11] or [31] for some approaches). The traditional classification of shapes is descriptive - supported by the drawing - and defines primarily the shape of the vessel as well as the shape of the rim and lip [9, 18]. In most publications, definitions of the terms shape, type and variant, are lacking. Subsequently, a subdivision based on subjective aspects is produced. The description of shape is subject to the ideas of the author and are not standardized. For examples see [5] and [23].

There have been attempts at description and classification based on mathematical definition of shape and type; a definition for which the relation of the diameter of the rim to the height of the vessel as well as the angle of inclination of the rim and wall are especially important [17].

A more formal scheme of ceramic classification has been described by Gardin [10, 11]. Individual features like the base, neck, and rim are compared with drawn examples and appropriately coded. Another method of classifying pottery is to define types in terms of ratios of the principal dimensions. An overview of such classification systems can be found in Millet [25] and Orton [27]. (In the course of a mathematical definition the description was omitted [14].)

The third way of classifying pottery is based on the examination of the methods of production by describing the steps taken to produce a vessel rather than classifying the finished product. Everything produced in the same way, that falls within the variations of shape that the particular technique permits, can be classified as one type [30]. The classification is a decision tree based on the traces left on the inner surface during production.

Traditional archaeological classification is based on the so-called profile of the object, which is the cross-section of the fragment in the direction of the rotational axis of symmetry. This two-dimensional plot holds all the information needed to perform archaeological research. The correct profile and the correct axis of rotation are thus essential to reconstruct and classify archaeological ceramics.

Figure 2 shows the inner side of a fragment on the left, its left side (broken surface) in the middle, and the profile section generated automatically on the right (Figure 1 shows the same fragment drawn by hand). The profile shown in Figure 2 was computed using a laser system and a shape from the structured light technique described in [21].



Figure 2: (a) Archaeological fragment - (b) site of fracture and - (c) profile section

The most formalized approach uses mathematical curves to describe the shapes of the vessels and their parts. The profile is thus converted into one or more mathematical curves. These approaches (i.e. the sampled tangent profile [24], the B-spline methods [16], the two-curve system [15]) provide the most precise representation so far, however no automatic comparison of complete profiles resulting from these methods have been published. The situation is complicated by the fact that ceramic vessels, produced by hand, do not have mathematically perfect surfaces which affects the application of the above mentioned methods and consequently, the precision of the representation of the vessels is reduced [28].

In this paper, we apply several methods for interpolation and approximation by *B*-splines on reconstruction of the vessel profiles (i.e. the profiles are projected into the plane). *B*-splines were chosen for the profile representation because they have a universal approximation property (i.e. for a given approximation error ϵ , there exists a *B*-spline constructed by means of a sufficiently large data set, so that the error of the approximation of the data by this function is at most ϵ , proven by [22]) and because they have a relatively simple mathematical definition.

By combining the different spline methods on subdivided intervals of the curve, the selection of the method with the best precision on a particular subdivision of the curve enables the detection of the significant 'non'-smooth parts of the curve. This (automatic) subdivision of the curve into intervals is done for two reasons. The first reason is that this division of a closed curve (i.e. not a function) is due to that any functional method can be applied. The second reason is that these boundary points of these intervals are at the same time important points for an archaeological analysis done by traditional methods (we suppose that the profile is given in correct orientation).

The *B*-spline methods are compared from the point of view of the approximation error (least mean square of the differences of the input value and the spline value) and from the point of view of the simplicity of the representation. The most appropriate method (in general, the combination of approximation and interpolation methods in single intervals), giving the smallest possible er-

ror and the simplest possible B-spline representation, is selected and the error of the whole 'reconstructed profile' with respect to the given data computed. This selection together with a demonstrative creation of the curve provides the archaeologist with as truthful as possible image of the reconstructed profile. The method was tested on profiles like shown in Figure 3.



Figure 3: Profiles of different fragments

The organization of the paper is as follows: Section 3 explains cubic splines. Selected interpolation methods are described and evaluated in Section 4 whereas Section 5 analyses approximation methods, while the selection of the unique method with the smallest approximation error and simplest representation is discussed in Section 6. The paper concludes with a discussion of the results presented and gives an outlook on future work.

2 Cubic Splines

The following definitions were adopted from [7]. We suppose that the planar closed curve \mathbf{r} (the profile of the vessel) to be fitted (interpolated or approximated) will be represented by parametric equations

$$\mathbf{r}(t) = [\mathbf{x}(t), \mathbf{y}(t)] \quad (1)$$

in an interval $\langle a, b \rangle$ in the Cartesian coordinates of \mathcal{R}^2 and has continuous second derivatives (i.e. r belongs to \mathcal{C}^2). The curve is given by a set of points $P_i = [x(t), y(t)]$ together with the non-decreasing sequence of knots $\{t_i; i = 1, \dots, n+1\}$ of parameter t (for which in the case of interpolation $x(t_i) = t_i; i = 1, \dots, n+1$). To construct a curve $S(t)$ which approximates the function given by the points (or for $t = t_i$ passes the points $P_i, i = 0, \dots, n+1$ - the interpolation case) can be done by constructing a cubic spline with an adequate parameterization and external conditions. The curve must be initially divided into sub-intervals where functional approximation and interpolation methods can be applied.

The support of a cubic spline is 5 intervals (i.e. elsewhere it equals 0). Denote by B_i^4 an k -th order spline ($k \leq 3$) whose support is $[t_i, t_{i+4}]$ (this contains 5 intervals created by the knot sequence). Then, it is possible to normalize these splines so that for any $x \in [a, b]$ holds $\sum_{i=-3}^{n+3} B_i^4(x) = 1$; Figure 4 shows the basis spline functions over knots t_{i-3}, \dots, t_i . It is clear that the sum of the splines over the 5 intervals equals 1.

Any cubic spline $S_n(x)$ with knots t_0, \dots, t_n and coefficients $a_{-3}, a_{-2}, \dots, a_n$ can be written in the

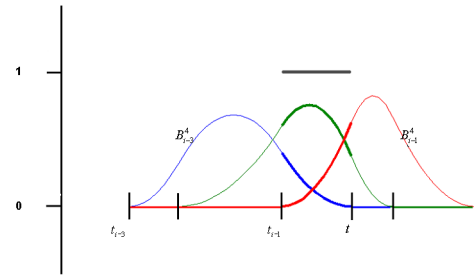


Figure 4: B-spline functions

form

$$S_n(x) = \sum_{i=-3}^n a_i B_i^4(x). \quad (2)$$

$B_i^4(x)$ is a polynomial of the degree at most 4 in each interval $\langle t_i, t_{i+1} \rangle$, elsewhere zero. To achieve a unique spline representation for a given data set and knots, the data must satisfy Schoenberg-Whitney Conditions (The arbitrary data at sites $x_1 < x_2, \dots, < x_n$ with the given knot sequence are matched by a spline uniquely, if and only if $B_i^4(x_i) \neq 0$ for all i). All our applied methods satisfy these conditions.

3 Interpolation by Cubic B-Splines

To solve the interpolation problem (i.e. an exact fitting of data points by a curve, see the Figure 5 below), we selected four methods which empirically showed up to be appropriate in our experiments:

- Cubic spline interpolation with Lagrange end-conditions (*cs1*) (i.e. it matches end slopes to the slope of the cubic that matches the first four data at the respective end);
- Cubic spline interpolation with not-a-knot end-condition (*cs2*);
- Spline interpolation with an acceptable knot sequence (*cs3*);
- Spline interpolation with an optimal knot distribution (*cs4*). As 'optimal' knot sequence the optimal recovery theory of Michelli, Rivlin and Winograd [4] is used for interpolation at data points $\tau(1), \dots, \tau(n)$ by splines of order k ;

These methods were applied to each of the intervals of the curve (into which the curve representing the profile is divided in order to any functional methods can be used), and their approximation error (least mean square of the differences of the input value and the spline value) was evaluated on the given data set.

All the discussed interpolation methods satisfy the Schoenberg-Whitney conditions, i.e. the

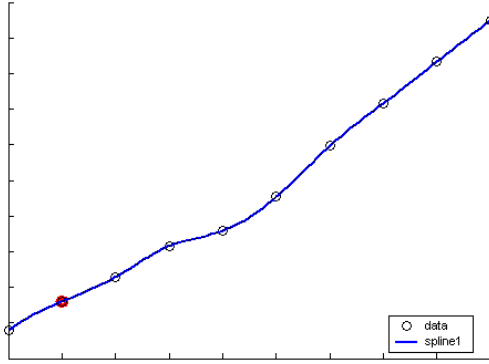


Figure 5: Interpolation by B-spline functions

achieved representation is for the method, the given data and knot sequences unique. The selection of a unique interpolation representation of the curve in the particular interval is made using the following criteria in the respective order:

1. Minimal approximation error in the corresponding interval.
2. Minimal length of the knot sequence
3. Priority of the interpolation method based on the statistical observations

The priority of the methods was achieved experimentally on profiles and their particular intervals as follows: 1. Cubic spline interpolation with Lagrange end-conditions (*cs1*); 2. Cubic spline interpolation with not-a-knot end-condition (*cs2*); 3. Spline interpolation with an acceptable knot sequence (*cs3*); 4. Spline interpolation with an optimal knot distribution (*cs4*).

4 Approximation by Cubic B-Splines

Since the amount of data pairs acquired to describe a vessel or its parts do not always suffice to represent the shape of the vessel reliably, interpolation does not have to be always the appropriate method. For this reason, we compared the approximation methods on representing the overall shape of the whole curve with respect to the interpolation methods. To solve the approximation method (i.e. an approximate fitting of data points by a curve with respect to a minimal approximation error over the interval from which are the data points taken, see Figure 6), we selected four methods which appeared as appropriate in our experiments. As in the interpolation case, the approximation error is measured as the least mean square of the differences of the input value and the spline value. The following approximation methods were applied and compared:

- a) Cubic smoothing spline with the smoothing parameter $p > 0$ (*cs5*); This smoothing spline f minimizes $p \sum_{j=1}^n w_j (y_j - f(x_j))^2 + (1-p) \int (f^{(2)}(t))^2$ with $w_j = 1, j = 1, \dots, n$, where n is the number of data points. (For $p = 0$, the smoothing spline is the least-squares straight line fit to the data, while, at the other extreme, i.e. for $p = 1$, it is the 'natural' or variational cubic spline interpolant.)
- b) Smoothing spline with the smoothing parameter $tol > 0$ (*cs6*); This function creates the smoothest function f in the sense that $F(f^{(2)}) = \sum \int_{x_1}^{x_n} (f^{(2)}(t))^2$ is the smallest, for which $E(f) = \sum_{j=1}^n w_j (y_j - f(x_j))^2 \leq tol$, with the weights $w_j = 1$ and data points $x_j, j = 1, \dots, n$ (where n is the number of data points.)
- c) Least squares spline approximation with the number of knots equal to a half of the amount of the data (*cs7*);
- d) Least squares approximation with the number of knots equal to the number of data - degree of the spline in the particular interval, (*cs8*);

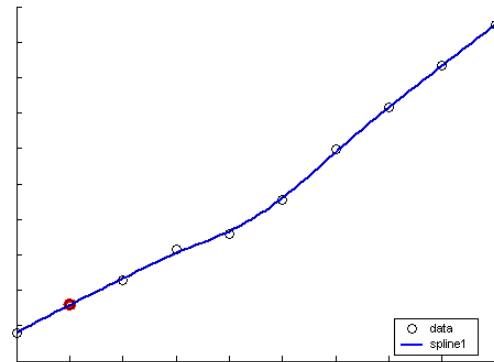


Figure 6: Approximation by B-spline functions

The approximation errors of both smoothing spline methods *cs5* and *cs6* vary with great differences, depending on the selection of the parameters $p > 0$ and $tol > 0$, respectively. A correct selection of p and tol can decrease the error over the interval, but there is no simple method for such selection known which would in general guarantee that the approximation error of the corresponding functions is minimal for such a choice of parameters. In the case of the cubic smoothing spline with parameter p (*cs5*), the selection of $p = 1$ gave a variational cubic spline interpolant (and thus 'low' errors with respect to the data). (As the setting of tol in the method *cs6* is more difficult, this method did not show up as appropriate

for creating an automated system, whose part the selection of the curve representation should be).

An 'optimal' (in the sense of the compared methods, given data and the applied criteria for selection) method is selected according to the same criteria as in the interpolation case and again, the priority ordering of the methods was achieved experimentally: 1. Cubic smoothing spline with the smoothing parameter $p > 0$ (*cs5*); 2. Smoothing spline with the smoothing parameter $tol > 0$ (*cs6*); 3. Least squares spline approximation with the number of knots equal to a half of the amount of the data (*cs7*); 4. Least squares approximation with the number of knots equal to the number of data - degree of the spline (*cs8*).

5 Results

When the most appropriate interpolation and approximation methods are computed and selected for each of the intervals of the curve, the method with a smaller error (in case of ambiguity, the interpolation method is preferred) is selected for the interval. The approximation error of the representation over the whole curve is computed. This representation is unique and optimal with respect to the above-mentioned criteria. The most frequently selected interpolation method was *cs1* and the most frequently selected approximation method was *cs6* in our experiments. An interpolation method was preferred in the intervals where a sufficient number of data with respect to the length of the interval was given. An approximation method was preferred in the intervals where there was a lack of data.

The process of applying all interpolation and approximation methods is displayed for every sub-interval of the curve after each run of the program (Figure 8 shows the methods applied on sub-interval no. 8). While the curve is generated gradually for each sub-interval of the curve, the overall approximation error is computed. The final picture of the profile constructed from the selected methods is displayed (Figure 9), and compared to the data set. Table 1 displays the approximation errors for all methods in all intervals of the profile from Figure 7, including the selected interpolation and approximation methods for the corresponding interval and the selected overall method for the whole profile. The whole data sets contained approximately 350 data points and the length of the whole curve was approximately 400 points.

6 Discussion and Conclusion

The method presented for selection of an 'optimal' representation (optimal with respect to the considered methods and selection criteria) of a (2-dim) profile of an archaeological fragment computes and displays a unique solution. The achieved fragment representations, the first part of an automated system for classification of archeological fragments, are the input of the second part of the system,

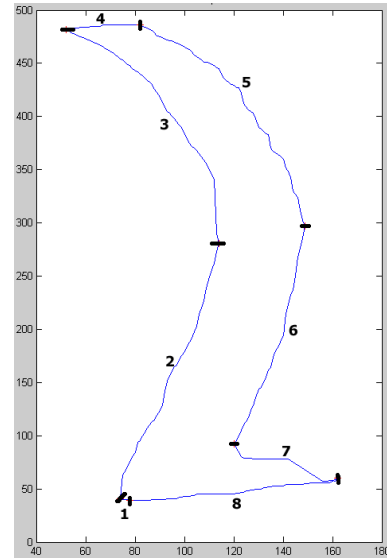


Figure 7: Computed profile subdivided into 8 intervals

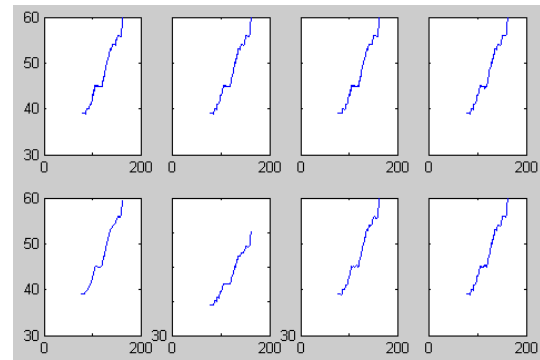


Figure 8: Interval nr. 8 computed with 8 different methods

classification. The profile parts - the so-called profile primitives are used to perform the classification. The segmentation (division) into primitives depends on the orientation of the fragment. In order to achieve a unique representation, it is important to set a unique orientation for all fragments. The classification will be solved in the high dimensional real space and therefore the uniqueness and the high precision of the profile representation are very important.

The classification will be solved in the high dimensional real space and therefore the uniqueness and the high precision of the profile representation are very important.

The method has been tested on synthetic and real data with good results. The current task is to meet the archaeological requirements as for the achieved representation.

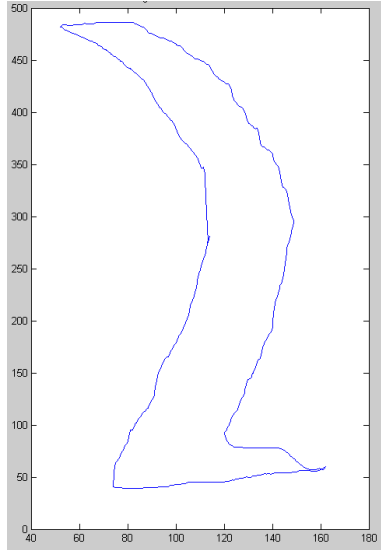


Figure 9: Glued intervals

| method / interval | 1 | 2 | 3 | 4 |
|-------------------|--------|--------|--------|---------|
| cs1 | 0.2163 | 0 | 0.6047 | 0.0781 |
| cs2 | 0.2163 | 0 | 0.5994 | 0.0782 |
| cs3 | 0.2163 | 0 | 0.5994 | 0.0782 |
| cs4 | 0.2163 | 0.6169 | 2.1080 | 0.0877 |
| cs5 ($tol = 5$) | 0.2163 | 2.3114 | 0.5994 | 1.1816 |
| cs6 ($p = 1$) | 0.1350 | 0 | 0.6229 | 0.07812 |
| cs7 | 0.2163 | 5.9470 | 5.5298 | 0.5015 |
| cs8 | 0.2163 | 0.0032 | 0.6014 | 0.1308 |
| select. intp. | 1 | 1 | 2 | 1 |
| select. appr. | 6 | 6 | 5 | 6 |
| overall select. | 6 | 1 | 2 | 1 |

| method / interval | 5 | 6 | 7 | 8 |
|-------------------|--------|--------|--------|--------|
| cs1 | 1.1685 | 2.2497 | 1.1424 | 0.0884 |
| cs2 | 1.1686 | 2.2514 | 0.1433 | 0.0884 |
| cs3 | 1.1686 | 2.2514 | 0.1430 | 0.0883 |
| cs4 | 1.4510 | 2.3485 | 0.1615 | 0.0991 |
| cs5 ($tol = 5$) | 2.9430 | 2.2514 | 2.2073 | 0.0884 |
| cs6 ($p = 1$) | 1.1687 | 2.2496 | 0.1646 | 0.0884 |
| cs7 | 6.9127 | 6.2323 | 0.8617 | 1.0675 |
| cs8 | 1.1850 | 3.8347 | 0.1430 | 0.2551 |
| select. intp. | 1 | 1 | 1 | 1 |
| select. appr. | 6 | 6 | 8 | 6 |
| overall select. | 1 | 6 | 1 | 6 |

Table 1: Approximation errors for all methods in all intervals

7 Acknowledgments

The authors would like to thank Prof. Marc Waelkens and Roland Degeest from the Katholieke Universiteit Leuven, Eastern Mediterranean Archaeology, Kristina Adler and Martin Penz from Vienna University, Institute of Classical Ar-

chaeology, and Raimund Kastler from Austrian Academy of Science, Institute for Studies of Ancient Culture for their archaeological support and contributions in evaluating the profile representation approach and for helpful and inspiring discussions.

References

- [1] W.Y. Adams and E.W. Adams. *Archaeological Typology and Practical Reality. A Dialectical Approach to Artifact Classification and Sorting*. Cambridge, 1991.
- [2] D.E. Arnold. *Ceramic Theory and Cultural Process*. Cambridge, 1985.
- [3] L.R. Binford. Archaeological Systematics and the Study of Cultural Process. *American Antiquity*, 31:203–210, 1965.
- [4] T.J. Rivlin C.A.Micchelli and S. Winograd. The Optimal Recovery of Smooth Functions. *Numerische Mathematik*, 26:191–200, 1976.
- [5] A. Carandini. Atlante delle forme ceramiche II, forma toynbee 1957. page 142, 1985.
- [6] W. Czysz and W. Endres. *Archäologie und Geschichte der Keramik in Schwaben*. Neusädf, 1991.
- [7] R. DeVore and G. Lorentz. *Constructive Approximation*. Springer, 1993.
- [8] W. Erdmann, H.J. Kühn, and H. Lüdtkke. Rahmenterminologie zur mittelalterlichen Keramik. pages 417–436, 1984.
- [9] E. Ettliger, P.M. Kenrick, K. Roth-Rubi, and S. Zabehlicky-Scheffenegger. *Conspectus formarum terrae sigillatae italico modo confectae*. Bonn, 1990.
- [10] J.C. Gardin. *Code pour l'analyse des ornements*. Paris, 1978.
- [11] J.C. Gardin. *Code pour l'analyse des formes de poteries*. Paris, 1985.
- [12] V. Gassner. Zur Entstehung des Typus der ionisch-massiliotischen Amphoren. In *Fremde Zeiten. Festschrift für Jürgen Borchhardt*, pages 165–176. Wien, 1996.
- [13] I. Gathmann. ARCOS, ein Gerät zur automatischen bildhaften Erfassung der Form von Keramik. *FhG - Berichte*, (2):30–33, 1984.
- [14] A. Guénoche and A. Tchernia. Essai de construction d'un modèle descriptif des amphores. In *Méthodes classiques et méthodes formelles dans l'étude des Amphores (Actes du colloque de Rome 27-29 Mai 1974)*, pages 247–259. École Française de Rome 32, 1977.

- [15] M.B. Hagstrum and J.A. Hildebrand. The two-curve Method for Reconstructing Ceramic Morphology. *American Antiquity*, 55(2):388–403, 1990.
- [16] N.S. Hall and S. Laffin. A Computer Aided Design Technique for Pottery Profiles. In S. Laffin, editor, *Computer Applications in Archaeology*, pages 178–188. Computer Center, University of Birmingham, Birmingham, 1984.
- [17] E. Hamon and A. Hesnard. Problèmes de documentation et de description relatifs à un corpus d’amphores romaines. In *Méthodes classiques et méthodes formelles dans l’étude des Amphores (Actes du colloque de Rome 27-29 Mai 1974)*, pages 17–33. École Française de Rome 32, 1977.
- [18] J. W. Hayes. Late Roman Pottery, London. page 61, 1972.
- [19] M. Kampel and R. Sablatnig. On 3d Modelling of Archaeological Sherds. In *Proceedings of International Workshop on Synthetic-Natural Hybrid Coding and Three Dimensional Imaging, Santorini, Greece*, pages 95–98, 1999.
- [20] M. Kampel and R. Sablatnig. Automated 3D Recording of Archaeological Pottery. In *D. Bearman and F. Garzotto (Ed.). Proc. of the Int. Conf on Cultural Heritage and Technologies in the Third Millennium Milan, Italy*, pages 169–182, 2001.
- [21] C. Liska and R. Sablatnig. Estimating the Next Sensor Position based on Surface Characteristics. In *International Conference on Pattern Recognition*, pages 538–541, September 2000.
- [22] A. Pinkus M. Leshno, V.Y. Lin and S. Schocken. Multilayered Feedforward Networks with a Nonpolynomial Activation Function can Approximate any Function. *Neural Networks*, 6:861–867, 1993.
- [23] M. Mackensen. Die spätantiken Sigillata- und Lampentöpfereien von El Mahrine (Nordtunesien). page 590, 1980.
- [24] P.L. Main. Accessing Outline Shape Information Efficiently within a large Database. In S. Laffin, editor, *Computer Applications in Archaeology*, pages 73–82. Computer Centre, University of Birmingham, Birmingham, 1986.
- [25] M. Millet. An Approach to the Functional Interpretation of Pottery. In *Pottery and the Archaeologist*, pages 35–48. London, 1979.
- [26] C. Orton, P. Tyers, and A. Vince. *Pottery in Archaeology*, 1993.
- [27] C.R. Orton. *Mathematics in Archaeology*. Cambridge, 1980.
- [28] P.M. Rice. *Pottery Analysis: A Sourcebook*, 1987.
- [29] R. Sablatnig and C. Menard. Computer based Acquisition of Archaeological Finds: The First Step towards Automatic Classification. In P. Moscati/S. Mariotti, editor, *Proceedings of the 3rd International Symposium on Computing and Archaeology, Rome*, volume 1, pages 429–446, 1996.
- [30] J.M. Schuring. Bulletin Antike Schaving. In *Studies on Roman amphorae I-II*, pages 59–137, 1995.
- [31] C.M. Sinopoli. *Approaches to Archaeological Ceramics*. New York, 1991.
- [32] C. Steckner. Das SAMOS Projekt. *Archäologie in Deutschland*, (Heft 1):16–21, 1989.
- [33] P. Waldhaeusl and K. Kraus. Photogrammetrie für die Archäologie. In Kandler M., editor, *Lebendige Altertumswissenschaft: Festgabe zur Vollendung des 70. Lebensjahres von Hermann Vetters dargebracht von Freunden, Schülern und Kollegen*, pages 423–427, Wien, 1985.